Leaf hydraulic maze; Differential effect of ABA on vascular bundle-sheath, palisade, and spongy mesophyll controlling hydraulic conductance

Adi Yaaran[1], Eyal Erez[1], Carl Procko[3] and Menachem Moshelion[1]*

[1] Institute of Plant Sciences and Genetics in Agriculture, The Robert H. Smith Faculty of Agriculture, Food and Environment, The Hebrew University of Jerusalem, Rehovot 76100, Israel.

[2] Plant Biology Laboratory, Salk Institute for Biological Studies, La Jolla, California 92037, USA.

***Corresponding author**:
Menachem Moshelion,
The Robert H. Smith Faculty of Agriculture, Food and Environment,
The Hebrew University of Jerusalem,
Rehovot, Israel
E-mail: menachem.moshelion@mail.huji.ac.il

Keywords

ABA, leaf hydraulics, spongy mesophyll, palisade mesophyll, bundle sheath, P_f

Running title: Differential effect of ABA on leaf hydraulic conductance.

ABSTRACT

Leaf hydraulic conductance (K_{leaf}) facilitates water for transpiration, enabling the continuation of CO_2 upsurge while maintaining water status. Nevertheless, radial water flow out-of-the-xylem and its regulation under well and stress conditions remain vague. We hypothesized that bundle-sheath and mesophyll cells play key roles in the radial flow of water out of the xylem and the regulation of that flow under optimal and stress conditions. We generated transgenic *Arabidopsis* plants that were insensitive to abscisic acid (ABA) exclusively in their bundle sheath (BSabi) or mesophyll (MCabi). BSabi plants showed greater K_{leaf} and transpiration under optimal conditions, with stomatal apertures and index and vein density like those of the wild type. MCabi exhibited even higher K_{leaf} and transpiration, as well as larger stomatal apertures, a higher stomatal index and greater vascular diameter and biomass, relative to the wild type. In response to xylem-fed ABA, both transgenic lines exhibited reduced K_{leaf} and transpiration, while their leaf water potentials remained unchanged. The greater osmotic water permeability (P_f) of the wild types' spongy mesophyll was reduced by ABA; whereas the lower P_f of the palisade mesophyll was not affected by ABA. Genetically modified, ABA-insensitive spongy mesophyll cells had a low P_f; whereas ABA-insensitive bundle-sheath cells had a higher P_f. The flow over the symplastic water pathway was increased by ABA, but its contribution to K_{leaf} was negligible. High levels of ABA appear to regulate the P_f of bundle-sheath and spongy mesophyll cells, to control K_{leaf}. Under optimal conditions, ABA limits transpiration and K_{leaf} via physiological, morphological, and developmental modifications of bundle-sheath and mesophyll cells. The bundle sheath–spongy mesophyll pathway controls K_{leaf} and leaf water balance under both optimal and drought conditions.

INTRODUCTION

The movement of CO_2 into the leaf and the loss of water from the leaf both occur through the stomata, creating a strong relationship between transpiration and productivity (de Wit, 1958; Fischer et al., 1998; Richards, 2000; Kemanian et al., 2005; Blum, 2009; Sperry et al., 2017; Sinclair, 2018; Xiong and Nadal, 2020). To support productivity (high transpiration), plants must efficiently conduct water from the soil to the evaporation sites on the leaf. Leaf hydraulic conductance (K_{leaf}) is a substantial bottleneck accounting for up to 98% of the total plant water resistance for well-watered plants (approx. 30% on average) (Sack and Holbrook, 2006). K_{leaf} is the ratio of water flow through the leaf (xylem to evaporation site) to the water potential gradient across the leaf (Sack and Holbrook, 2006). K_{leaf} is a dynamic trait, that responds to both abiotic (Tyree et al., 2005; Blackman et al., 2009; Shatil-Cohen et al., 2011; Pou et al., 2013; Prado and Maurel, 2013; Sadey et al., 2015; Kelly et al., 2017) and biotic stress (Attia et al., 2019; Dalal et al., 2020). The structural-functional regulation of leaf hydraulics is viewed as a system made up of four main pathways: 1) hollow xylem elements; 2) the apoplast, along the cell walls of the leaf tissues; 3) the symplast, which connects cells via plasmodesmata and 4) transmembrane transport, mainly via aquaporins (AQPs). Eventually, the water evaporates at the cell-wall surface and exits the leaf as vapor through the stomatal pore. However, little is known about the relative contributions of the different pathways and the mechanisms that regulate K_{leaf}.

A simplified approach divides K_{leaf} into two parts: xylem hydraulic conductance, K_x, known as the axial path, and out-of-xylem hydraulic conductance, K_{ox}, known as the radial path. Leaf vein architecture and density greatly affect K_x (Nardini et al., 2005a; Brodribb et al., 2007; Blackman et al., 2010; Brodribb et al., 2010; Scoffoni et al., 2011; Caringella et al., 2015). As the xylem vessels are composed mainly of dead cells, rapid K_{leaf} impairment was previously attributed to breaks in the water-column continuum (i.e., embolism). However, in recent decades, research has revealed that living cells are involved in the regulation of K_{ox}, which makes a significant contribution to K_{leaf} (Shatil-Cohen et al., 2011; Sade et al., 2014; Scoffoni and Sack, 2017; Grunwald et al., 2021).

The living vascular parenchyma, bundle-sheath cells (BSC) and mesophyll cells (MC) can potentially regulate K_{ox} according to internal and environmental signals. High resistance of K_{ox} may also help leaves to avoid catastrophic xylem failure (Scoffoni et al., 2017) by dynamically regulating the resistance of the "next in line" pathway (Yaaran and Moshelion, 2016). Previously, stress-induced changes in K_{ox} were attributed to leaf shrinkage (i.e., physical alterations of the apoplastic water pathway; Scoffoni et al., 2014)

and/or to changes in AQP expression and/or activity (i.e., alterations in the transmembrane water pathway). The latter has been reported in BSC (Kim and Steudle, 2009; Shatil-Cohen et al., 2011; Prado et al., 2013; Sade et al., 2015), MC (Morillon and Chrispeels, 2001), guard cells (Grondin et al., 2015) and the whole leaf (Nardini et al., 2005b; Cochard et al., 2007; Pou et al., 2013; Kelly et al., 2017).

The bundle sheath is a single cell layer enwrapping the vasculature, which possesses selective barrier characteristics (Pilot et al., 2004; Leegood, 2008; Galvez-Valdivieso et al., 2009; Grunwald et al., 2021) with low apoplastic transport (Shapira et al., 2009; Shatil-cohen and Moshelion, 2012). It is symplastically isolated from the xylem, which constrains the transmembrane movement of water into the leaf, but is connected to neighboring MC by plasmodesmata (Ache et al., 2010). The anatomical structure of the MC correspondingly affects K_{leaf} (Brodribb et al., 2007; Scoffoni et al., 2014; Buckley, 2015). The current assumption is that the palisade MC function as a sort of water capacitor (Zwieniecki et al., 2007), while the spongy MC are more dynamic in terms of their water status, playing a significant role in the determination of K_{ox} (Buckley, 2015; Xiong and Nadal, 2020). In MC, water can move via all three pathways in parallel. A controlled trade-off between water pathways has been suggested as a mechanism for coping with drought stress (Morillon and Chrispeels, 2001), yet supportive evidence for this hypothesis is scarce, suggesting routing toward the apoplastic pathway (Pou et al., 2013) or an increase in transmembrane pathway (Morillon and Chrispeels, 2001; Martre et al., 2002).

The drought-induced phytohormone abscisic acid (ABA) has been shown to reduce the membrane osmotic water permeability (P_f) of BSC via AQPs (Shatil-Cohen et al., 2011), demonstrating controlled trade-offs between the transmembrane water pathway and regulation of K_{leaf} via non-stomatal mechanisms (Pantin et al., 2013; Coupel-Ledru et al., 2017). ABA increased the P_f of WT Arabidopsis mesophyll protoplasts after 24 h, but not after 1–5 h (Morillon and Chrispeels, 2001; Shatil-Cohen et al., 2011). Only a few works have studied the effects of abiotic stress on plasmodesmata. Those works have reported inconsistent results regarding increased (Erwee and Goodwin, 1984; Schulz, 1995) and reduced (Cui and Lee, 2016; Kitagawa et al., 2019) permeability of the plasmodesmata. We, therefore, hypothesized that ABA might have a direct effect on the symplastic water pathway, in addition to its effect on the transmembrane water pathway.

In addition to its widely studied role as a stress hormone, low basal levels of ABA have recently been shown to play a major role in physiological and developmental mechanisms related to plant water status (reviewed by Yoshida et al., 2019), setting a steady-

state stomatal aperture (Merilo et al., 2018; Yaaran et al., 2019). However, to the best of our knowledge, the effects of basal ABA on K_{leaf} and, particularly, on K_{ox} have not yet been investigated.

The general goal of the current study was to improve our understanding of the leaf hydraulic maze, particularly along the BSC and MC continuum. We hypothesized that K_{ox} is dynamically regulated by the BSC and MC symplastic, transmembrane and apoplastic pathways, in a manner that is controlled by ABA levels, from low basal ABA levels (under optimal growth conditions) to higher ABA levels in response to stress. To test this hypothesis, we constructed tissue-specific ABA-insensitive plants (*abi1-1* mutant gene under tissue-specific promoter), MCabi (MC ABA-insensitive plants (Negin et al., 2019) and BSabi (BSC ABA-insensitive plants), both of which maintained a WT-like stomatal response to ABA. We addressed the effects of the tissue-specific insensitivity to ABA from the cellular level through whole-plant transpiration rates.

MATERIALS AND METHODS

Plant Material and Growing Conditions

All of the *Arabidopsis thaliana* plants used in this study were of the Colombia (col) ecotype (wild type; WT). In addition to WT plants, we also used transgenic FBPase::*abi1-1* (MCabi; Negin et al., 2019) and SCR::*abi1-1* (BSabi) plants. *CalS8-1* (037603C) was generously provided by Jung-Youn Lee and *AtBG_ppap* (SAIL_115_G04) was ordered from SALK (Loughborough UK). PCR was used to confirm the homozygosity of both of those lines. *CORI3::GUS-mCit* and *IQD22::GUS-mCit* lines were constructed by Carl Procko (Procko et al., 2022) and were crossed with MCabi2 to generate lines with ABA-insensitive, labeled spongy or palisade MC. Labeling of the bundle sheath was done by crossing BSabi14 with *SCR::GFP* (Torne et al., 2021).

Arabidopsis plants were grown in 250-mL pots, with two to three plants in each pot. Those pots were filled with soil (Klasmann686, Klasmann-Deilmann, Germany) + 4 g/L Osmocote® 6M. The potted plants were kept in a growth chamber at 22°C and 70% relative humidity, with an 8-h light (09:00 – 17:00) /16-h dark photoperiod (short-day). During the day, the illumination, humidity and vapor pressure deficit (VPD) changed in a pattern resembling natural conditions, as in (Negin and Moshelion, 2017). The illumination intensity provided by LED light strips [EnerLED 24 V-5630, 24 W/m, 3000 K (50%)/6000 K (50%)] reached 150–200 μmol m^{-2} s^{-1} at the plant level at midday.

The FBPase::*abi1-1* and SCR::*abi1-1* Constructs and Plant Transformation

For construct assembly, the MultiSite Gateway Three-Fragment Vector Construction Kit (Invitrogen) was used according to the manufacturer's instructions. The construction of the MCabi mesophyll ABA-insensitive plants is described in Negin et al. (2019) (In that work, MCabi plants are referred as *fa* plants.) Briefly, the *abi1-1* gene (Koornneef et al., 1984) and the FBPase promoter (Lloyd et al., 1991) were cloned into pDONR plasmids and then inserted into the binary pB7M24GW (Invitrogen, Ghent Belgium) plasmid. As MC and BSC are connected by plasmodesmata, we cannot exclude the diffusion of mutated *abi1-1* genes from MC to BSC. Therefore, we considered MCabi plants to be ABA-insensitive in their MC and BSC. The bundle sheath ABA-insensitive (BSabi) plants were constructed in the same way, using the SCR (Shatil-Cohen et al., 2011) promoter, which has been observed in the BSC associated with all veins in mature leaves (Wysocka-Diller et al., 2000). We cannot rule out the diffusion of *abi1-1* into other tissues in BSabi plants, yet trans-activation of a hairpin by an enhancer trap (J1511) active in the leaf veins showed silencing moved only 2–7 cells away from the vein (Janacek et al., 2009). Binary plasmids were floral-dipped (Clough and Bent, 1998). The presence of the transgene containing the G to A substitution was confirmed by sequencing and NocI digestion (described below). The study was performed on three independent lines of each construct, using homozygous t_3 and t_4 lines.

Characterization of Transgenic Plants

Stomatal Aperture and Index

Stomatal aperture and index were measured as described by Yaaran et al. (2019). Briefly, epidermal peels were soaked in ‘closure’ solutions under light (~150 μmol m^{-2} s−1). After 1.5 h, ABA ((+)-cis, trans abscisic acid; Biosynth; Staad, Switzerland) was added to reach a concentration of 10 μM. DMSO at the same concentration was added to the control. All stomata were photographed under a bright-field inverted microscope (1M7100; Zeiss; Jena, Germany) on which a Hitachi HV-D30 CCD camera (Hitachi; Tokyo, Japan) was mounted. Stomatal images were analyzed to determine aperture size using the ImageJ software. Stomatal index was calculated as the number of stomata / number of epidermal cells.

Leaf Vein Density

Leaf vein density was measured as described by Grunwald (2021a). Briefly, leaves of the same age and size as those used in the K_{leaf} assay were immersed in 96% (v/v) ethanol solution and incubated at 50°C. The used ethanol was replaced with fresh ethanol until leaves

were completely colorless and then was finally replaced with 88% (v/v) lactic acid solution (Fischer Scientific, UK) for overnight incubation at room temperatuere. Then, the leaves were rinsed in water and submerged in 0.5% safranin O dissolved in water (Sigma Aldrich cat. No S2255) for 1 min, followed by an overnight incubation in water to remove any excess dye. Then, the leaves were scanned in a water tray using an Epson 12000XL scanner (Seiko Epson, Japan) with a 2500-dpi resolution and two to three patches of each leaf (9–10 leaves per line) were analyzed using WinRhizo™ software (https://regent.qc.ca/assets/winrhizo_about.html) for vein detection. Vein density was calculated by dividing the total vein length by the total leaf area scanned.

Rosette and leaf area were measured as described by Negin et al. (2019). Scans were performed using an Epson Perfection v37 scanner (www.epson.com).

Leaf cross-sections for anatomical analysis of the veins and mesophyll were free-hand cut using a sharp scalpel. Then, the cross-sections were cleared using ClearSee (Kurihara et al., 2015) and stained in a 1-min incubation in Toluidine Blue O dissolved in water (TB; cat.#: T-3260, https://www.sigmaaldrich.com). They were then washed with water two or three times. Cross-sections were photographed in the same set-up as that used for the analyses of stomatal aperture and index. Images were analyzed to determine length and are using the ImageJ software.

Leaf Gas-Exchange and Hydraulic Conductance (Kleaf) Measurements

Gas exchange and hydraulic conductance were measured as described by Negin et al. (2019), using leaves of 6- to 8-week-old plants grown under short-day conditions. Briefly, two leaves from each plant were excised pre-dawn and put into tubes containing AXS (Shatil-Cohen et al., 2011) and 0.01% DMSO (control) or 10 μM ABA. The leaves were then put into hermetically sealed transparent boxes and left in the light for a minimum of 1 h. Following that period, the lids were opened for 15 min, after which time gas exchange was measured using the LI-6400xt portable gas-exchange system (LI-COR, Inc., Lincoln, NE, USA). Chamber conditions were set to 400 ppm CO2, PAR of 200 μE m−2s−1, VPD of ~1.2 and flow of 200 μmol/s. In the enclosed gas-exchange chamber there is a trade-off between the stability of humidity vs. stability of the flow. We choose to keep constant flow on the expense of humidity stability to keep an undisturbed boundary layer. Immediately following the gas-exchange measurement, the leaf was transferred to a pressure chamber (ARIMAD-3000; MRC Israel) to measure Ψ_{leaf} and determine K_{leaf} (Sade et al., 2014). K_{leaf} was calculated for

each individual leaf by dividing the whole-leaf transpiration rate, E, by the leaf water potential (Martre et al., 2002; Sack and Holbrook, 2006). In our calculation, leaf water potential equals Ψ_{leaf} measured by pressure chamber as the leaf petiole was dipped in AXS at a water potential of 0. These measurements were conducted between 10:00 and 13:00 (1–4 h after the lights were turned on).

Whole-Plant Continuous Transpiration

The whole-plant continuous transpiration rate was measured using a high-throughput telemetric, gravimetric-based phenotyping system (Plantarry 3.0 system; Plant-DiTech, Israel; Dalal 2020) in the greenhouse of the I-CORE Center for Functional Phenotyping (http://departments.agri.huji.ac.il/plantscience/icore.phpon) as described in (Yaaran et al., 2019; Dalal et al., 2020). The output (weight) of the load cells was monitored every 3 min and analyzed using SPAC analytics (Plant-Ditech, Israel). Seedlings were transferred to 1.6-L pots (four plants per pot) and gradually exposed to greenhouse semi-controlled conditions: 24–9°C (day/night) and natural day length and light conditions prevailing in Rehovot, Israel during December and January of 2021.

After establishment, each pot was placed on a load cell in a randomized block arrangement. Daily measurements were conducted continuously and simultaneously for all of the plants in the array, so that all of the plants were exposed to similar ambient conditions at each measurement point. The soil surface surrounding each Arabidopsis plant was covered, as well as the crack between the pot and load cell, to prevent evaporation. The transpiration rate was normalized to the total plant weight, to determine E as described in (Halperin et al., 2016; Yaaran et al., 2019).

Protoplast Isolation and Measurement of the Membrane Osmotic Water Permeability Coefficient (P_f)

Protoplast isolation and measurements of the osmotic water permeability coefficient (P_f) were performed as described by Shatil-Cohen et al. (2014). In brief, protoplasts were isolated from 6- to 8-week-old plants according to the gentle and rapid (<30 min) method using an isotonic solution in the extraction process (pH 5.7, 600 mOsmol). For the ABA treatment, protoplasts were incubated in 1 μM ABA for 1–4 h. We observed the protoplasts swelling in response to hypo-osmotic challenge (of 0.37 MPa) generated by changing the bath solutions from isotonic (600 mOsmol) to

hypotonic (450 mOsmol). Palisade and spongy mesophyll protoplasts were identified by *mCit* fluorescence. Protoplasts were recorded using an inverted epifluorescent microscope (Nikon Eclipse TS100) with a 20x/NA 0.40 objective, a CCD 12-bit camera Manta G-235B (https://www.alliedvision.com) and image-processing software (AcquireControl® v5.0.0; https://www.alliedvision.com). P_f was determined based on the rate at which cell volume increased for 60 s starting from the hypo-osmotic challenge using a numerical approach, in an offline curve-fitting procedure of the PfFit program.

Relative Symplastic and Apoplastic Permeability

Drop and See (DANS) Assays

Drop and see (DANS) assays were performed as described by Cui and Lee (2016) with minimal modifications. In brief, two 1-µL droplets of 2 mM 5(6)-carboxyfluorescein diacetate (CFDA; cat. #19582 https://www.caymanchem.com) were loaded on the center of the adaxial surface of a mature leaf from a 7- to 8-week-old plant. This was followed by inverted epifluorescent microscope imaging (detailed above, P_f measurements) of the abaxial surface of the leaf 10 min after loading. The non-fluorescent ester CFDA can cross cell membranes passively in its electrically neutral or near-neutral form. Once inside the cells, it is subject to cleavage by esterases to form a polar fluorescent compound, CF. The extent of cell-to-cell dye movement is expected to represent the permeability of the plasmodesmata and was evaluated using an Intensity-Distance chart that was analyzed using ImageJ. The average of the two droplets was considered the leaf's DANS measurement.

Apoplastic Flow Ratio

The apoplastic flow ratio was determined by the polar apoplastic variant 5(6)-carboxyfluorescein (CF; cat. #: 10269590 https://www.fishersci.de/de/de/home.html). To introduce CF dye into the tissue with minimal wounding, the leaf was pricked twice (on the left and right sides of the mid-vine) with a sterilized acupuncture needle (0.16 × 40 mm), resulting in uniform radial injuries (Suppl. Fig. 6C). Two 1-µL droplets of 0.1 mM CF were placed directly on the wound. The experimental set-up was the same as that used for the DANS assays and the average for the two droplets was considered as the leaf relative apoplast permeability.

Both attached and detached leaf measurements were performed between 10:00 and 14:00. The detached-leaf experimental set-up was like the set-up used for the measurements of hydraulic conductivity (K_{leaf}).

Statistical Analysis

The data were analyzed using Student's *t*-test for comparisons of two means and the Tukey-Kramer test for comparisons of more than two means. All analyses were done using JMP software (SAS; Cary, NC, USA).

RESULTS

Characterization of the BSabi and MCabi Phenotypes

To better understand the effects of ABA on leaf hydraulics, we generated tissue-specific ABA-insensitive lines. We expressed the dominant *abi1-1* mutation under the FBPase promoter (for expression in green tissues, but not in guard cells) to create plants that were insensitive to ABA in their MC and BSC (i.e., MCabi plants) or under the SCR promoter (for expression in BSC, but not in MC) to construct plants with BSC that were insensitive to ABA (i.e., BSabi plants; see Materials and Methods). Three independent lines were selected for each (MCabi1, 2, 7 and BSabi12, 14, 99).

The MCabi plants were broadly characterized and validated (Negin et al., 2019) and the same validation was performed for the BSabi plants (Suppl. Fig. 1). MCabi and BSabi lines exhibited different phenotypes, illustrating the vital implications of expression location. MCabi's rosette size, leaf size and thickness were greater than those of the WT, while those of BSabi were smaller (Fig. 1A–D, E–H). BSabi maintained the same proportion of palisade to spongy MC as the WT; whereas MCabi had more space occupay by palisade MC (Fig. 1E–H). Despite the changes in leaf size, the vein densities of BSabi and MCabi remained the same as that of the WT (Fig. 1I–L), with BSabi differing from WT in its smaller veins and MCabi in its larger proportion of xylem to total vein area (Fig. 1M–P). Moreover, the stomatal index (Fig. 1Q–T) and steady-state stomatal aperture (Fig. 1U–X) of MCabi were greater than those of the WT and BSabi. Both MCabi and BSabi plants had a WT-like stomatal response to ABA (Negin et al., 2019; Suppl. Fig. 1C) and their average foliar ABA levels were similar to those of the WT (Suppl. Fig. 2A; one of the three BSabi lines had ABA levels that were higher than those of the WT; Suppl. Fig. 2B).

Gas Exchange and Leaf Hydraulics

To assess the relative contributions of the MC and BSC to the overall K_{leaf}, we performed gas-exchange measurements and then measured Ψ_{leaf} using a pressure chamber. Under optimal conditions, BSabi and MCabi had similar levels of transpiration (E), which were higher than that of the WT. Yet, despite that higher E, both transgenic plants maintained Ψ_{leaf} that was similar to that of the WT, resulting in higher K_{leaf} than WT (Fig. 2A–C). BSabi and MCabi exhibited higher stomatal conductance (g_s) and slightly higher A_N, resulting in lower water-use efficiency (iWUE; Fig. 2D–F). Following ABA treatment, all lines exhibited reduced E and K_{leaf} and the differences between the lines were preserved (Fig. 2A, B). However, only WT showed a reduction in Ψ_{leaf} (despite its E being much smaller than those of the transgenic plants, Fig. 2B). This resulted in the overall higher WUE of the WT, as compared to the two sets of transgenic lines, even following ABA treatment (Fig. 2F).

Although MCabi plants had a higher stomatal index and larger stomatal apertures than BSabi (Fig. 1Q, U), they had the same E and g_s (Fig. 2A, D). Gas-exchange measurements of E were performed in an enclosed gas-exchange chamber, in which it was difficult to maintain a constant VPD under high E (Suppl. Fig. 3). To overcome this challenge, we measured whole-plant transpiration under natural conditions using a gravimetric system in which all plants were simultaneously exposed to the same VPD. We found that MCabi plants had highest transpiration rate (Fig. 3E). This trend was maintained throughout the whole growing period (40 days: Suppl. Fig. 4C). When transpiration was normalized to the plant's weight, MCabi still had the highest E, with BSabi exhibiting intermediate-level E and WT exhibiting the lowest E (Fig. 3F). These results unveil the additive impact of the mesophyll on the leaf water balance.

Differences Between the Palisade and Spongy MC: P_f and ABA Response

To study the mesophyll's contribution to E and K_{leaf}, in general, and the specific contributions of palisade and spongy MC, we used reporter lines with palisade (*IQD22pro::GUS-mCit*) and lower spongy (*CORI3::GUS-mCit*) tissue-specific labeling with the fluorescent protein mCit. The two reporter lines reveal largely restricted labeling as we did not find any apparent labeling on any other leaf tissue including bundle sheath and guard cells under our conditions (Fig. 4A, B). Spongy mesophyll protoplasts exhibited higher P_f under control conditions (Fig. 4C) and were

smaller than the palisade protoplasts (Fig. 4D). The P_f values of both types of protoplasts showed a "tailed distribution" with most of the protoplasts having low P_f values. Yet, even when considering only 90% of the population, in order to exclude the "tails" of the populations, the P_f of the spongy mesophyll protoplasts remained almost double that of the palisade protoplasts. Moreover, far more spongy mesophyll protoplasts had extreme P_f values of over 60 µm sec^{-1}. In response to ABA, the higher P_f of the spongy mesophyll protoplasts was reduced by roughly 60% (19.2 $\pm$ 0.7 µm s^{-1} to 7.2 $\pm$ 1.8 µm s^{-1} respectively), while the average P_f of the palisade protoplasts did not change (Fig. 4E).

To examine the effect of ABA insensitivity on MC, we fluorescence-labeled palisade and spongy mesophyll protoplasts of MCabi and found that ABA insensitivity reduced the P*f* of the spongy mesophyll protoplasts, but did not affect the palisade protoplasts (Fig. 4F). In contrast, bundle-sheath insensitivity to ABA resulted in increased P_f (Fig. 4G). After evaluating the transmembrane water pathway, we investigated the symplastic and apoplastic water pathways.

Effects of ABA on the Symplastic and Apoplastic Water Pathways

First, we were interested in evaluating the relative contribution of the symplastic water pathway to the total K_{leaf}. To that end, we measured the K_{leaf} of known mutants with severely impaired plasmodesmatal permeability: *CalS 8-1*, whose plasmodesmatal permeability is ~35% higher than that of the WT (Cui and Lee, 2016), and *AtBG_ppap*, whose plasmodesmatal permeability is ~45% lower than that of the WT (Zavaliev et al., 2013). The K_{leaf} values of both mutants were similar to that of the WT (Fig. 5A). Next, we measured the relative plasmodesmatal permeability of MCabi and BSabi under control conditions and in response to ABA treatment. Under control conditions, the relative plasmodesmatal permeability of the MCabi plants was highest, that of the BSabi was intermediate and the WT had the lowest relative plasmodesmatal permeability (Fig. 5B). Following ABA treatment, only WT leaves exhibited significantly increased relative plasmodesmatal permeability (Fig. 5B). the changes in relative plasmodesmatal permeability were not accompanied by any changes in detected callose levels (Suppl. Fig. 5B). Validation of proper callose staining was done on leaves pre-treated with flagellin, whose reduced relative plasmodesmatal permeability was accompanied by increased callose deposition, as expected (Suppl. Fig. 6A, B).

Evaluation of apoplastic flow was challenging, as the apoplast fluorescent dye (CF) did not penetrate the leaf surface and also could not penetrate the selective barrier of the BSC when fed through the petiole. Moreover, petiole feeding of CF may bias differences between the ABA treatment and the control, as CF is a pH-dependent fluorescent dye and ABA affects the pH of the xylem sap (Torne et al., 2021). To overcome that obstacle, a very small wound was made using an acupuncture needle (15 μm ± 0.7, see Materials and Methods), through which CF was introduced into the apoplast (Suppl. Fig. 6C). The relative apoplast permeabilities of the WT and BSabi were similar and greater than that of MCabi and were not affected by the ABA treatment (Fig. 5C).

DISCUSSION

BSC and MC Control K_{leaf} and Transpiration via ABA Regulation

The working hypothesis in this study was that K_{ox} is controlled by a series of living cells, including BSC and MC. Our results support this hypothesis and also show that spongy mesophyll P_f plays a major role in regulating K_{leaf} under both optimal and stress conditions. Moreover, the increased E and K_{leaf} observed among both BSabi and MCabi under optimal conditions implies that, in the WT, E and K_{leaf} are limited by a non-stomatal mechanism, most likely the effects of basal ABA on physiological and developmental regulation.

Recently, it was suggested that the basal levels of ABA expressed under non-stress conditions may limit the steady-state stomatal aperture to less than its potential maximal size (Merilo et al., 2018; Yaaran et al., 2019). Our finding that BSC insensitivity to ABA results in higher P_f (Fig. 4G) together with BSabi's elevated K_{leaf} (Fig. 2C) suggest that ABA may play a similar role in BSC-specific regulation. We suggest that this dual restricting role (in the guard cells and BSC) of basal ABA serves to preserve leaf water balance by balancing leaf water influx (via bundle sheath) and efflux (via guard cells) while increasing the P_f of spongy MC (Fig. 4F), to sustain overall water flow and content between the controlled entry and exit positions. We further suggest that this role of basal ABA is augmented by its activity under stress conditions, when high ABA levels reduce both stomatal apertures and K_{leaf}. Consequently, our results combined with previous studies in the literature lead us to suggest an ABA productive-survival feedback model (Fig. 6). It is interesting to note that similarities between the regulation mechanisms of guard cells and BSC have also

been reported in the context of blue light signal-transduction pathways, which initiate stomatal opening while increasing bundle sheath P_f (Iino et al., 1985; Zait et al., 2017; Torne et al., 2021; Grunwald, 2022). Our findings also reinforce the importance of the BSC as a leaf hydraulic checkpoint (Ache et al., 2010; Griffiths et al., 2013; Caringella et al., 2015).

Our suggested model does raise a question regarding the benefits to restricting hydraulic conductance (and possibly productivity) under optimal growth conditions. The answer to this question may come from the results showing that the unrestricted BSabi and MCabi plants exhibited reduced WUE. This is due to a major increase in E, as compared with the WT [168–180% under controlled growth-chamber conditions (Fig. 2A) and 68–80% under open-air greenhouse conditions (Fig. 3F)]. Meanwhile, the carbon assimilation rate, A_N, increased by only about 10% (Fig. 2E), supporting the suggestion that the photosynthetic system is saturated at high K_{leaf} levels (Brodribb et al., 2005). Thus, optimized WUE is likely to be stable in the non-maximal gas-exchange range (Yoo et al., 2009).

Under stress conditions, our results indicate that BSC and MC contribute to Ψ_{leaf} regulation as both BSabi and MCabi plants lack a Ψ_{leaf} response to ABA (Fig. 2B). This supports the ABA signaling-participating model, which suggests that stressed-induced xylem ABA affects stomatal closure via a non-stomatal mechanism (Pantin et al., 2013) by reducing BSC P_f , which reduces K_{leaf} while stomata remain open, reducing Ψ_{leaf}^{x}. Accordingly, BSabi's higher K_{leaf}, E and g_s (Fig. 2), even under ABA treatment, can be attributed to the high P_f of its BSC (Fig. 4G), which allows it to overcome its reduced xylem-to-veins ratio (Fig. 1M). MCabi's very high transpiration (Fig. 3, Suppl. Fig. 4) can also be explained by its morphology (e.g., increased ratio of xylem to veins, higher stomatal index and larger stomatal apertures; Fig. 1M–X), as well as the higher P_f of its BSC and the reduced P_f of its spongy mesophyll (Fig. 4F, G). These changes sustain high axial (K_x), as well as high radial (K_{ox}) water conductance and higher stomatal pathway.

Palisade and Spongy MC Differ in Their Hydraulic Properties

Palisade and spongy MC differ in both their structure and their hydraulic properties (Fig. 4; (Canny, 2012; Buckley et al., 2015; Álvarez-Arenas et al., 2018; Muries et al., 2019)). The smaller spongy MC are distant from each other, forming a tissue with large air spaces and low cell-to-cell connectivity (Buckley et al., 2015;

Borsuk et al., 2022). Based on our findings, the P_f of the spongy MC under non-stressed conditions was twice that of the palisade MC (Fig. 4C, E, F), possibly compensating for the structural challenges of water flow through that tissue and supporting its important role in K_{ox} (Buckley et al., 2015; Xiong and Nadal, 2020). The spongy mesophyll's vast exposure to the leaf's internal air spaces together with the high P_f of its cells may also explain those cells' rapid loss of water and shrinkage in response to high VPD (Canny, 2012) or dehydration (Muries et al., 2019). This is an intriguing point that may demonstrate how a change in the physical environment (i.e., low VPD) can be differentially transformed by the high P_f of the spongy MC into a decrease in water content, which alters cell-wall and plasma membrane interactions to induce ABA production (Bacete et al., 2022) and drive stomatal regulation accordingly (Yaaran and Moshelion, 2016; Sack et al., 2018; Fig. 6). This cellular regulation may also play an important role under drought conditions, when the leaf water balance deteriorates and ABA levels increase (Holbrook et al., 2002; Christmann et al., 2005). The sharp decline in the spongy MC's P_f in response to stress-induced ABA, while the palisade P_f remained unchanged (Fig. 4C) supports a role for the spongy MC in the dynamic regulation of K_{ox} and in the recently suggested dynamic regulation of the humidity gradient in the leaf air spaces (Wong et al. 2021). Moreover, it also highlights tissue-specific ABA regulation. The fact that the P_f of the palisade MC does not respond to ABA suggests a "static" hydraulic role for it (Zwieniecki et al., 2007), in which it serves as a water buffer to maintain leaf water balance (Nardini et al., 2010; Rockwell et al., 2014). The combination of palisade mesophyll with "static" hydraulic properties and the lack of any direct effect of ABA on photosynthesis (Negin et al., 2019) can be an advantage for continued photosynthesis (Tholen et al., 2012; Buckley, 2015) and positions ABA as, primarily, a water-balance regulator (from BSC to guard cells) controlling the transmembrane water pathway. Yet ABA also plays a role in regulating the symplastic water pathway.

The Role of Plasmodesmata in the Symplastic Water Pathway and K_{ox}

To evaluate the roles of plasmodesmata and the symplastic water pathway in K_{leaf}, we used impaired plasmodesmata-permeability mutants (*cals8-1*; (Cui and Lee, 2016) and *AtBG_ppap*; (Zavaliev et al., 2013)). Both of those mutants exhibited WT-like K_{leaf} (Fig. 5A), indicating that the symplastic pathway has a negligible influence on K_{leaf}. Moreover, the fact that ABA treatment increased the WT's symplastic

permeability (Fig. 5B), alongside its reduction of K_{leaf}, supports this indication. To explain this seemingly contradictory role of ABA, we suggest that under stress conditions, symplastic water flow may provide better cell-to-cell conductivity and turgor sharing, and also help to maintain a uniform water potential across all of the cells in the tissue. Additionally, it may act as a rapid facilitator of the stress signal by distributing the ABA itself in between the cells. These potentially beneficial traits of ABA remain to be confirmed and further research is required to determine the effects of ABA on plasmodesmata permeability.

Finally, we examined the apoplastic pathway, which is the flow of water within the cell walls according to the applied potential gradient. When the potential gradient is stronger toward the abaxial side, as in the case of MCabi's larger stomatal apertures and higher stomatal index (Fig. 1Q, U), and there is much stronger transpiration (Fig. 3F, Suppl. Fig. 4C), the spread of apoplastic dye is limited (Fig. 5C), since each stoma generates vertical water movement on the expanse of radial horizontal expansion (Rockwell and Holbrook, 2017). Consequently, the spread of the dye is more indicative of the direction of apoplastic flow than the volume of that flow and does not necessarily reflect the apoplast's contribution to radial water flow.

A Suggested Model for the Role of ABA in K_{leaf} Regulation

Integrating our results, we suggest the following model of radial water movement within the out-of-xylem leaf tissues (Fig. 7). Under optimal conditions, water enters the leaf through the BSC, which selectively regulate transmembrane radial water flux (Leegood, 2008; Galvez-Valdivieso et al., 2009; Shapira et al., 2009; Ache et al., 2010; Shatil-Cohen et al., 2011; Prado and Maurel, 2013; Grunwald et al., 2021) based on their membrane osmotic water permeability (Fig. 4G). Thus, the BSC barrier serves as the first control point regulated by basal ABA (Fig. 7A, control point 1). Then, water proceeds toward and within the MC with most flow occurring through the hydraulically dynamic spongy MC (Fig. 4C; Buckley et al., 2015; Buckley, 2015; Xiong and Nadal, 2020). The transmembrane pathway (Cochard et al., 2007; Kim and Steudle, 2007) and the apoplastic pathway (Sack and Holbrook, 2006; Voicu et al., 2009; Buckley, 2015) govern K_{leaf} under optimal conditions, while the contribution of the symplastic pathway is negligible (Fig. 5A–B, Fig. 7A, control point 2). The high P_f of the spongy MC may allow the spongy mesophyll to serve as an interchange point between the parallel water pathways, as water crossing the cell membrane may continue

toward the next cell in the transmembrane pathway or remain in the apoplast, leading to more wetting of the cell wall and supporting the apoplastic water pathway (Maurel, 1997; Steudle and Peterson, 1998; Fig. 7A, control point 3, 7B) and transpiration (Fig. 3F, Suppl. Fig. 4). The simultaneous limitation of K_{leaf} and stomatal aperture by basal ABA levels maintains the balanced water status in the leaf that is mirrored in the high Ψ_{leaf} and turgor (Fig. 6A).

Under limited-water conditions, a high level of ABA in the xylem reduces the BSC's P_f (Shatil-Cohen et al., 2011; Fig. 7C, control point 1), which limits the movement of water into the leaf. In the short term, the stomatal efflux remains unchanged and the higher initial P_f of the spongy MC (Fig. 4C) results in their water loss, shrinkage (Canny et al., 2012; Muries et al., 2019) and ABA production (McAdam and Brodribb, 2016; Sussmilch et al., 2017; Sack et al., 2018; Bacete et al., 2022; Fig. 6A, B). The higher levels of ABA then decrease the P_f of the spongy MC (Fig. 4E, Fig. 7C, control point 2, Fig. 6B), resulting in the retention of water within the whole mesophyll tissue and reducing the flow over the transmembrane water pathway, cell-wall wetting and, subsequently, the apoplastic flow (Fig. 7C control point 3, 7D). Reduced water conductance of the apoplastic and transmembrane pathways increases the MC's relative contribution to the total K_{leaf}. As a result of all the above and the direct effect of high ABA levels on stomata, K_{leaf} and g_s decrease, while leaf water status deteriorates (e.g., decreased turgor and Ψ_{leaf}; Fig. 6B). Simultaneously, the high ABA levels increase the symplastic permeability (Fig. 5B; Fig. 7C, control point 2), possibly facilitating the cooperation of mesophyll cells and solute transport when E levels are low (Morillon and Chrispeels, 2001).

This study highlights the differential effects of ABA on BSC and spongy and palisade MC, as well as newly reported effects of those tissues on K_{leaf}. Our efforts to untangle the effects of ABA on leaf hydraulics revealed that K_{ox} is controlled by a sequence of living cells, which are differentially affected by ABA. Moreover, we also provide evidence supporting a new role for ABA as a central water-balance coordinator under both optimal and stress conditions and suggest that ABA levels have a feed-back effect on leaf water status, dynamically fine-tuning leaf water influx and efflux in response to environmental changes.

Acknowledgments and Funding

This research was supported by ISF (the Israel Science Foundation, Grant No. 1043/20) and NIH (Grant No. 5R35GM122604). We thank Jung-Youn Lee for generously providing us with the *CalS8-1* (037603C) line. We thank Dr. Julius Ben-Ari for the LC-MS/MS analyses of ABA samples and Eduard Belausov for the confocal imaging.

Author Contributions

Adi Yaaran designed and performed the research, analyzed the data, formulated the hypotheses and wrote the manuscript. Erez Eyal contributed to the characterization of transgenic plants and P_f measurements. Carl Procko constructed and validated the *CORI3::GUS-mCit* and *IQD22::GUS-mCit* lines. Menachem Moshelion (the corresponding author) formulated the hypotheses and wrote the manuscript together with Adi Yaaran.

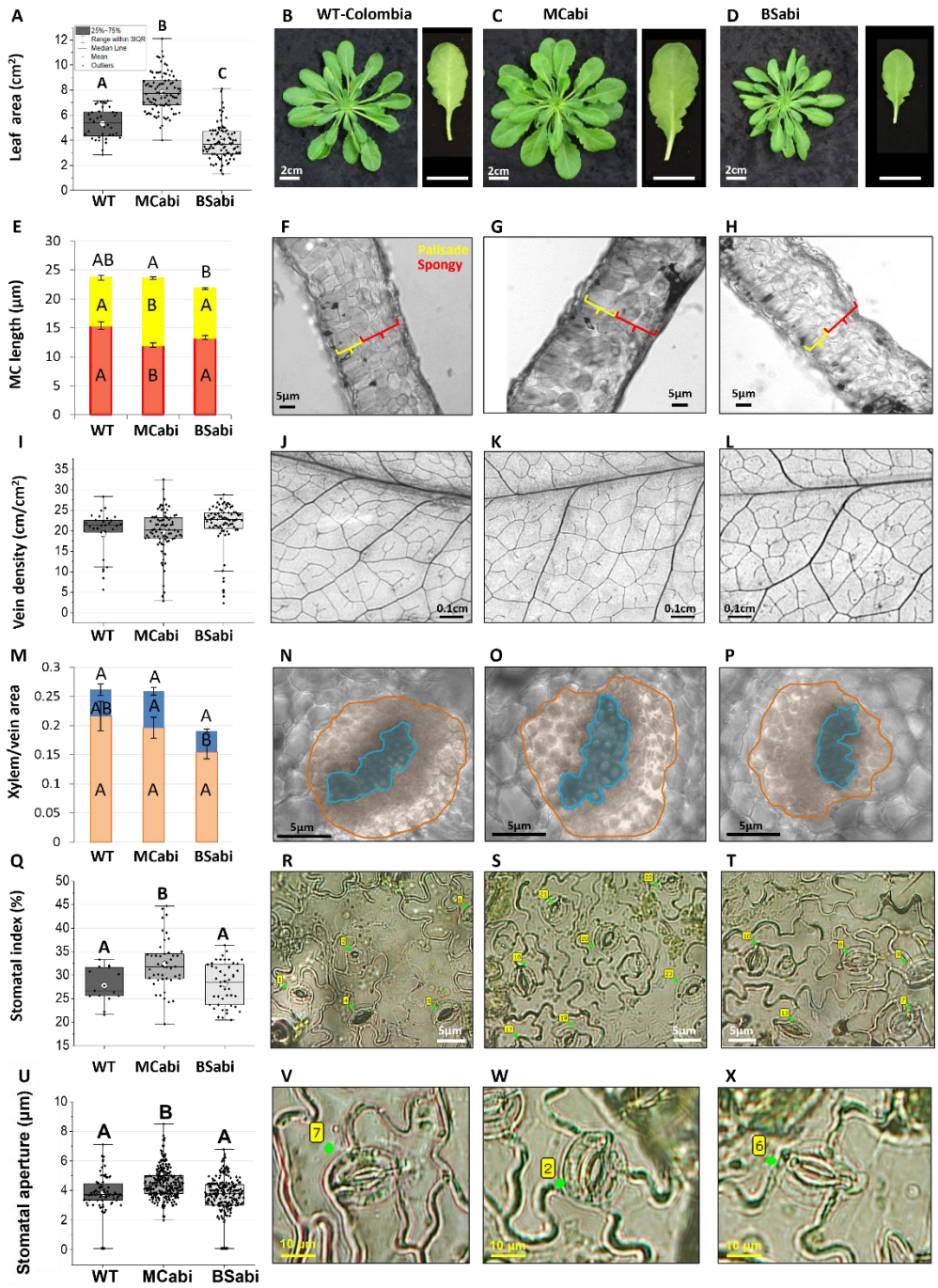

Figure 1. MCabi and BSabi phenotypes. Morphological characteristics of 7- to 8-week-old MCabi and BSabi plants grown under short-day conditions, including: (A) leaf area, (E) leaf thickness and the width of the palisade mesophyll (light gray, defined by yellow line) and the width of the spongy mesophyll (dark gray, defined by red line), (I) vein density, (M) the proportion of xylem (blue line in V–X) to total vein area (orange line in V–X), (Q) stomatal index and (U) stomatal aperture. Representative images of each measurement for the WT (B, F, J, N, R, V), MCabi (C, G, K, O, S, W) and BSabi (D, H, L, P, T, X) lines are also shown. Bar length is stated in each image. (A, E. I. M) The box height shows 25–75% of the data range, the symbols indicate the individual data values, the solid line indicates the median, o indicates the mean and the whiskers delimit ±3 times the interquartile range. (E, M) Data are means ± SE. Different letters indicate statistically different means (Tukey's test $P < 0.05$) of at least three independent experiments. (A: n = 36–90; E, M: n = 5–15 leaves, average of 3 cross-sections per leaf, 5 leaves for each transgenic line; I: n = 30–80; Q: n = 15–45 leaves; U; n = 80 > stomata.)

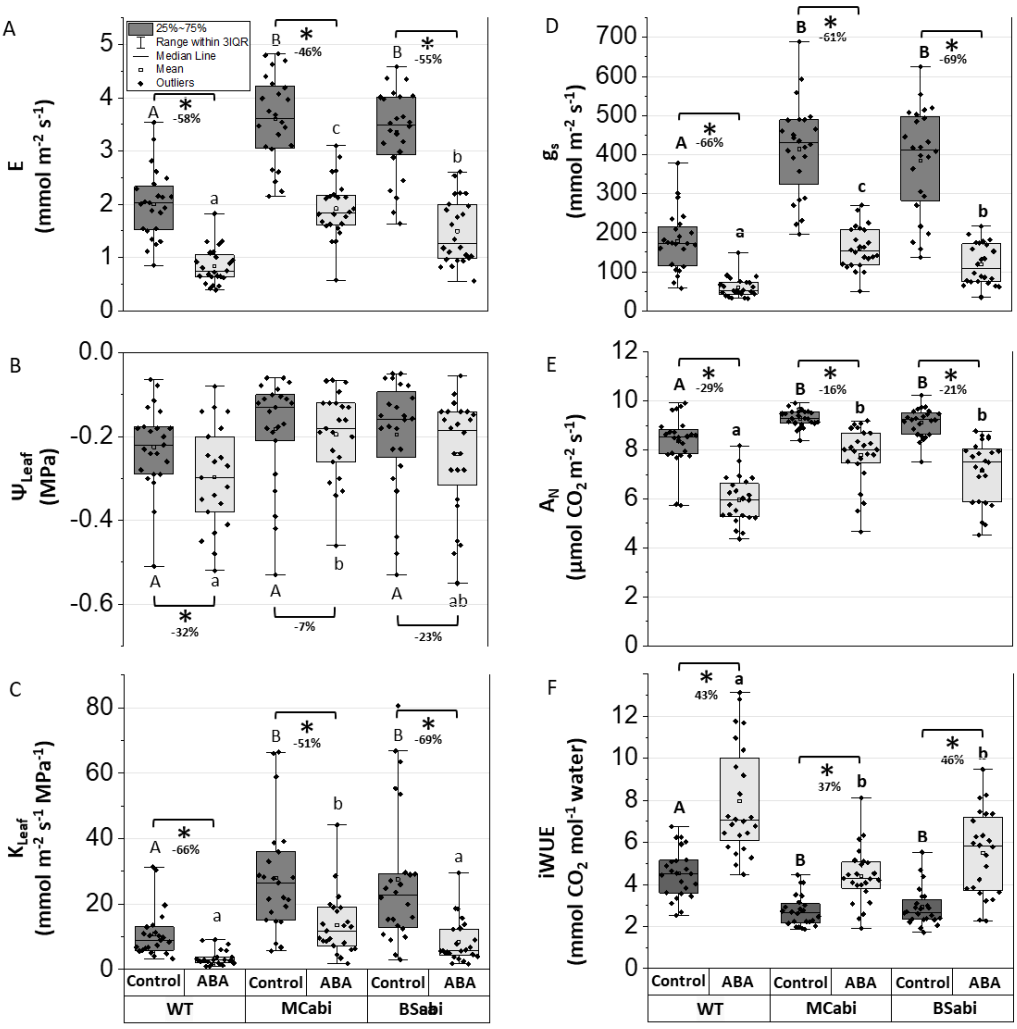

Figure 2. Leaf gas exchange of WT, MCabi and BSabi under non-stressed conditions in the presence of xylem-fed ABA. Leaves of 6- to 8 week-old plants were cut pre-dawn and fed through the petiole with AXS (dark gray) or with AXS + 10 µM ABA (light gray). After 1–4 h, the (A) whole-leaf transpiration rate, E, and (B) leaf water potential, Ψ_{leaf}, were measured, enabling the calculation of (C) leaf hydraulic conductance (K_{leaf}) for each individual leaf. In addition, the (D) stomatal conductance, g_s, and (E) net assimilation rate, A_N, were measured, enabling the calculation of (F) iWUE for the same leaves. The percentage change following the ABA treatment is indicated as well. Different letters indicate significant differences between genotypes within a treatment (capital letters for control and lower-case letters for ABA treatment) according to Tukey's HSD test. An asterisk indicates a significant difference between treatments within a genotype according to Student's *t*-test ($P < 0.05$). The box height shows 25–75 % of the data range, the symbols indicate individual data values, the solid line indicates the median, o indicates the mean and the whiskers delimit ±3 times the interquartile range of at least three independent experiments (n = 21–24).

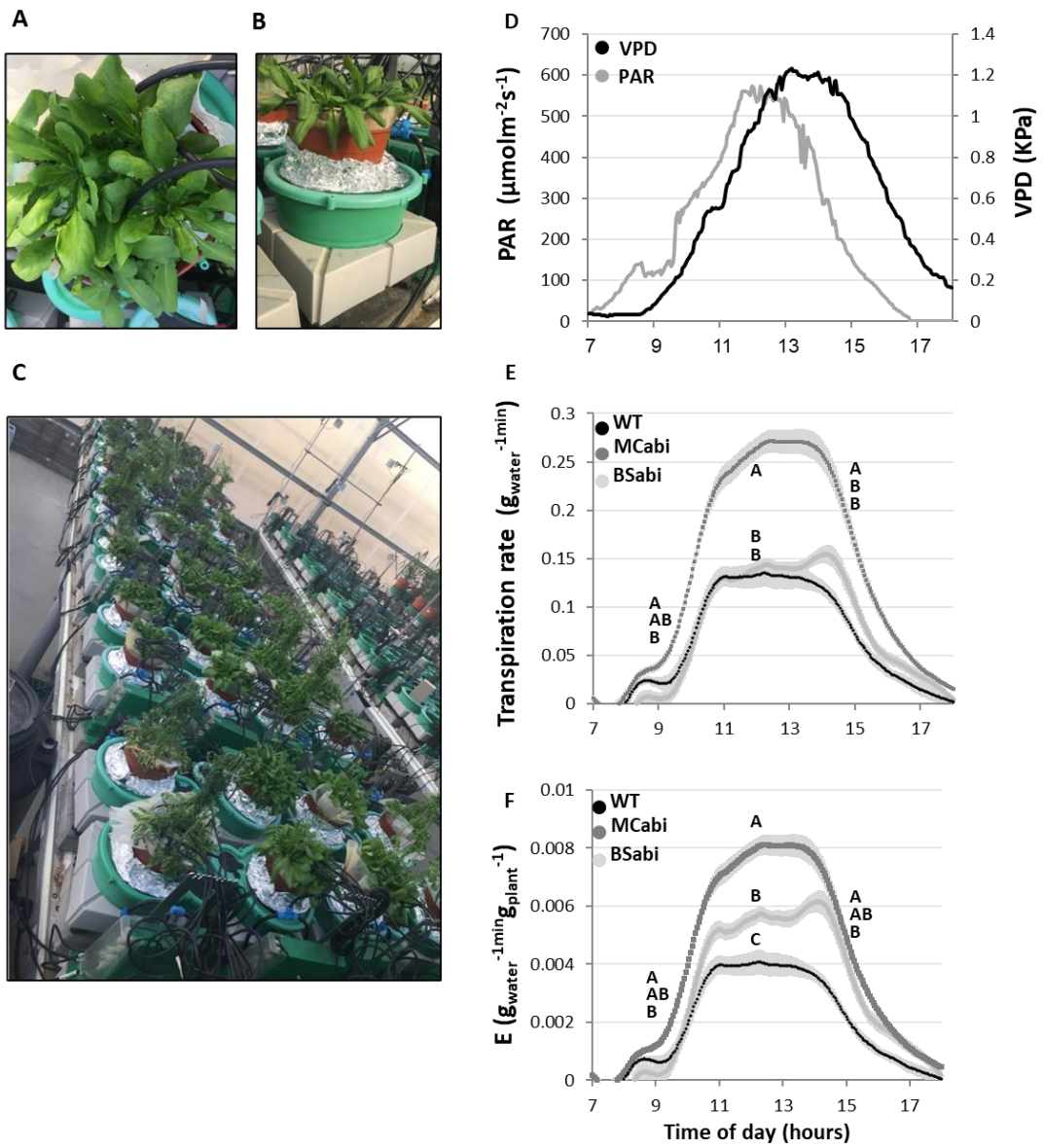

Figure 3. Continuous measurements of whole plants under greenhouse conditions. (A) Top view and (B) side view of pots with 8-week-old WT Arabidopsis plants, 4 plants per pot. All pots were randomized and simultaneously measured on (C) a lysimeter system located in a greenhouse under semi-controlled conditions. The plants were exposed to (D) ambient VPD and PAR conditions as shown here for one representative day. (E) Whole-plant continuous transpiration rates of WT (black), MCabi (dark gray) and BSabi (light gray). (F) Transpiration of the different lines, normalized to plant weight. Data are means + SE (WT: n = 5 pots; MCabi: n = 19 pots; BSabi: n = 18 pots; 4 plants in each pot). Letters indicate significant differences according to Tukey's test ($P < 0.05$) calculated at 09:00, 12:00 and 15:00.

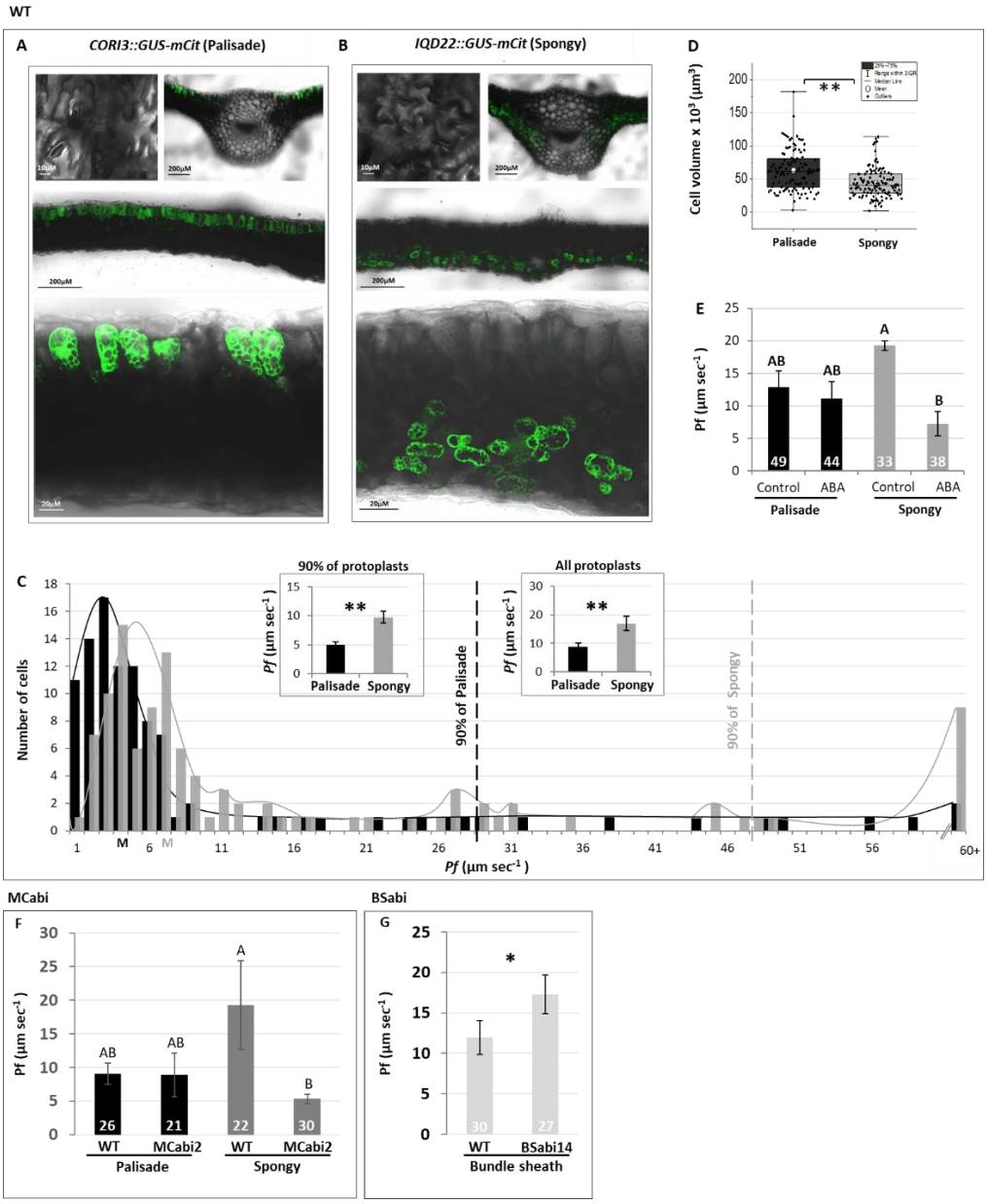

Fig. 4. Osmotic water permeability coefficients (*Pf*) of palisade-mesophyll and spongy-mesophyll protoplasts. (A) Fluorescent images of the stomata and cross-sections of *Arabidopsis* leaves expressing a GUS-mCitrine reporter protein under palisade or (B) spongy MC specific promoters (IQD22 and CORI3 promoters, respectively); bar sizes are shown in the images. (C) *Pf* distributions of WT palisade (black) and spongy (gray) MC protoplasts generated from IQD22::GUS-mCit and CORI3::GUS-mCit reporter lines, respectively. Dashed lines define the 'tail' of the top 10% outstanding *Pf* values of the 'high-*Pf*' for both types of protoplasts (>28 µm s^{-1} for palisade and >47 µm s^{-1} for spongy). Means ± SE of 90% of the populations are also shown. M – median. (D) Volumes of palisade (gray) and spongy (black) protoplasts; the box height shows 25–75% of the data range, the symbols indicate individual data values, the solid line indicates the median, o indicates the mean and the whiskers delimit ±3 times the interquartile range. (E) *Pf* response to pre-treatment with 1 µM ABA (1–4 h). (F) *Pf* of ABA-insensitive palisade and spongy mesophyll protoplasts and (G) ABA-insensitive bundle-sheath protoplasts (carrying the BSC marker SCR::GFP) under non-stress conditions. Data are means ± SE if not mentioned otherwise from at least 7 independent experiments for A–E and 4 independent experiments for F–G. Different letters indicate significant differences according to Tukey's test ($P < 0.05$) and asterisks indicate significant differences according to one tailed Student's *t*-test (*$P < 0.05$, **$P < 0.01$, C; spongy *Pf* higher then palisade D; palisade largere then spongy G; BSabi14 *Pf* higher then WT).

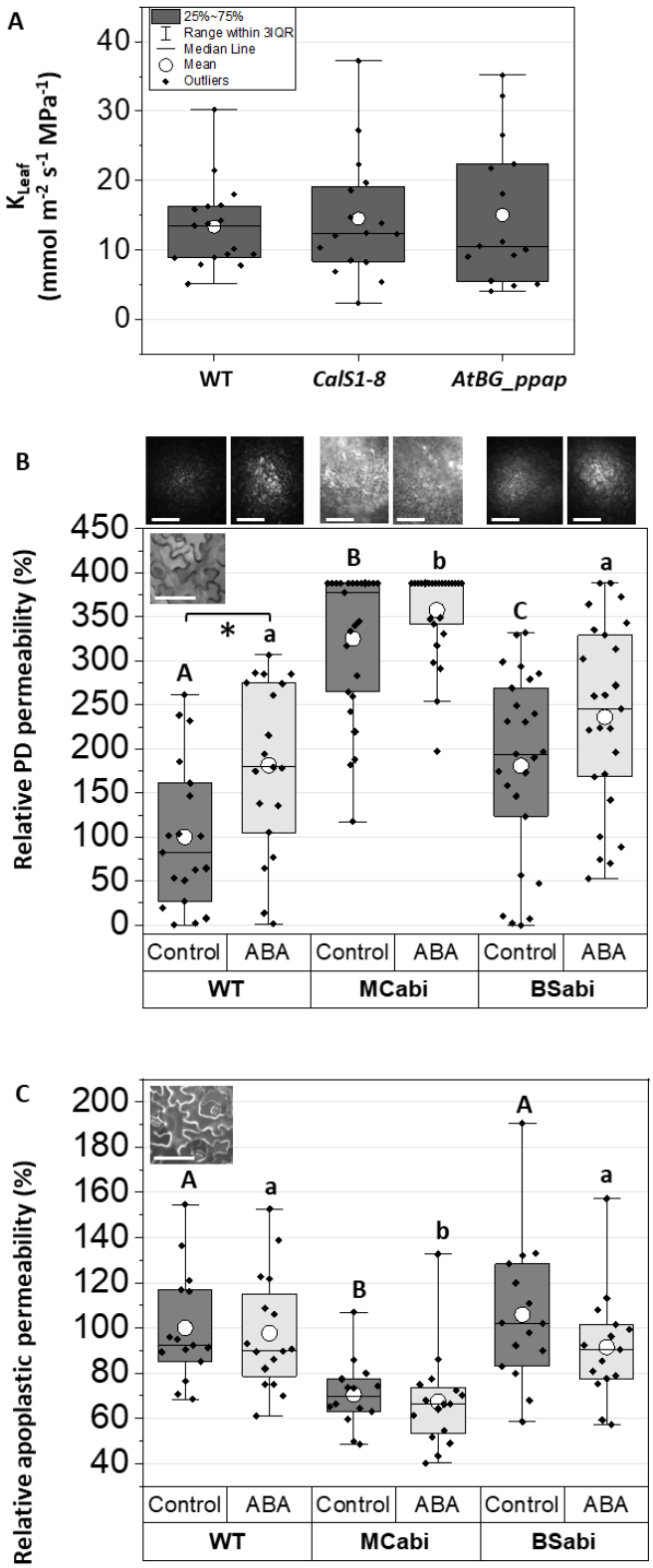

Fig. 5. Effects of ABA on the symplastic and apoplastic pathways. (A) K_{leaf} of mutants with impaired plasmodesmatal (PD) permeability. (B) DANS assays show the cell-to-cell movement of CF in WT, MCabi and BSabi plants that were petiole-fed AXS (dark gray) or AXS +10 µM ABA (light gray). Top: Representative images of cytoplasmic distribution of the CF dye (bar = 20 µm), as well as a close-up image showing that the dye was trapped within the cells (bar = 5 µm). (C) Apoplastic CF dye movement (MCabi2 and BSabi12, one line for each genotype). Top: A close-up image showing that the dye was trapped outside the cell. The box height shows 25–75% of the data range, the symbols indicate the individual data values, the solid line indicates the median, o indicates the mean and the whiskers delimit ±3 times the interquartile range. Different letters indicate significant differences between genotypes within a treatment (capital letters for control and lower-case letters for ABA treatment) according to Tukey's test. An asterisk indicates a significant difference between treatments within a genotype according to Student's *t*-test ($P < 0.01$). A: n = 15–17 leaves; B: n = ≥19; C: n = 15 leaves.

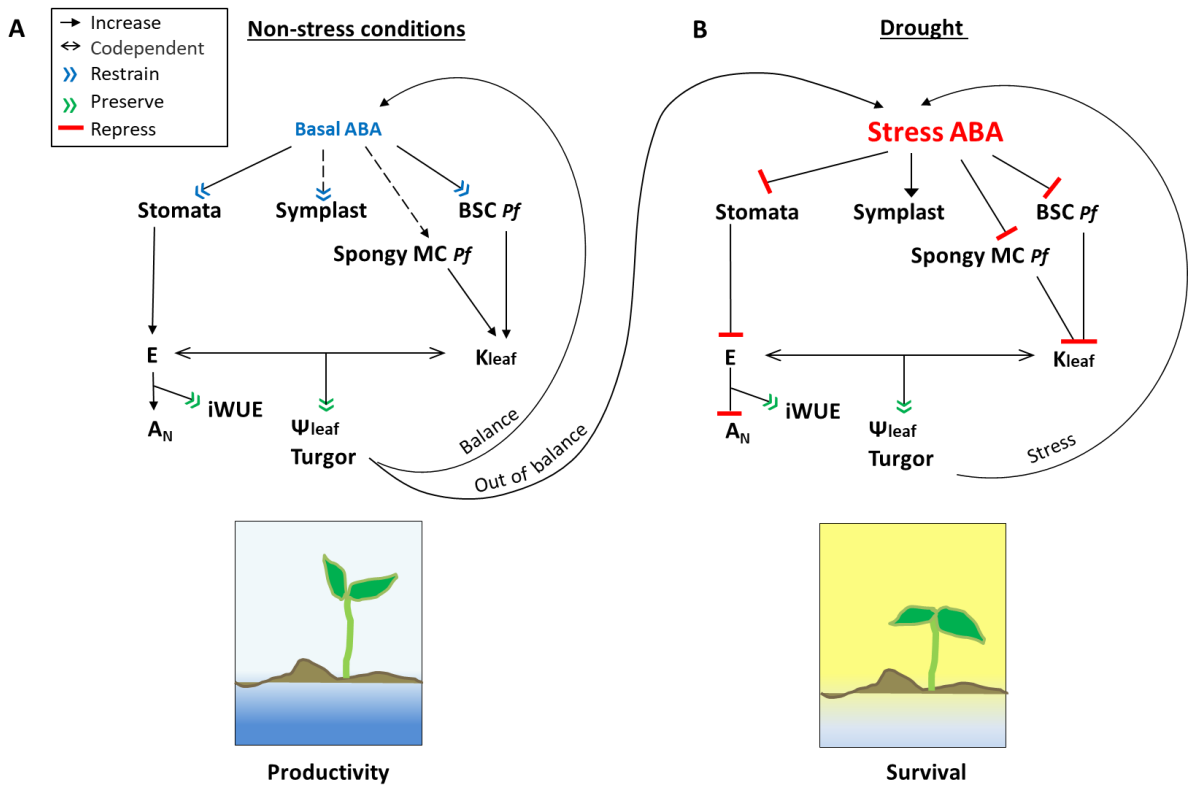

Fig. 6. ABA productivity–survival feedback model. (A) Under optimal ambient conditions, basal ABA levels limit maximal K_{leaf} through BSC *Pf*, as well as stomatal maximal steady-state aperture (Merilo et al., 2018; Yaaran et al., 2019), while increasing the transmembrane water flow through the spongy MC and cell-wall wetting. Balanced leaf water influx (K_{leaf}) and efflux (E) preserve leaf water status (Ψ_{leaf}, turgor and iWUE) and maintain carbon fixation (A_N). In turn, the leaf Ψ_{leaf} and/or turgor affect ABA levels, so that a balanced water status and low basal levels of ABA are maintained under optimal conditions. Violation of the balanced water status induces an increase in ABA levels (McAdam and Brodribb, 2016; Sussmilch et al., 2017; Sack et al., 2018; Bacete et al., 2022) and shifts the plant into a stress mode. (B) Stress-induced high levels of ABA reduce the BSC Pf (Shatil-Cohen et al., 2011), decreasing the flow of water into the leaf (at this initial time point, stomatal water efflux is relatively high). This further impairs the balance between water influx (Kleaf,) and efflux (E) and deteriorates the leaf water status (Ψleafand turgor). Such deterioration in leaf water status may also occur in response to a sudden increase in VPD, which reduces the turgor and Ψleaf. of the spongy MC (Canny et al., 2012), due to their high initial Pf. Low leaf water status amplifies the stress signal and increases ABA levels. Simultaneously, ABA increases the flow through the symplastic water pathway, yet its contribution to K_{leaf} seems negligible. The direct effect of ABA on stomata combined with reduced K_{leaf} diminishes E and, subsequently, water loss, as well as A_N. Through this sequence of events, the leaf water balance coordinates leaf water supply and demand with environmental fluctuations with greater efficiency, but lower productivity (i.e., higher iWUE)

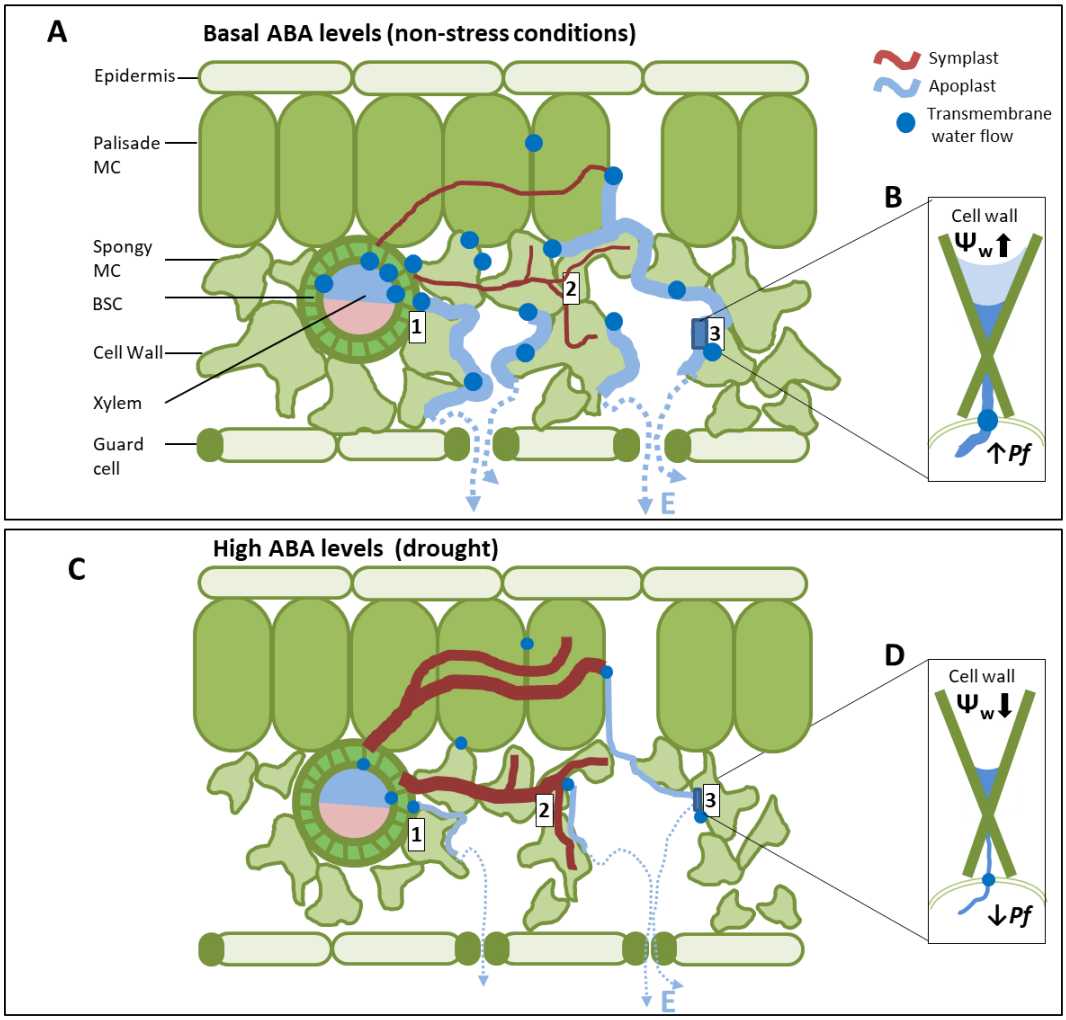

Fig. 7. A suggested model for ABA's regulation of K_{leaf}. (A) Under optimal conditions, water flows across the BSC barrier via the transmembrane water pathway, probably through aquaporins (blue dots; control point 1), and proceeds toward the mesophyll. In the mesophyll, water may flow in parallel pathways and move between the three pathways, The apoplastic (light blue line) and transmembrane pathways are dominant, while the contribution of the symplastic path (dark-red line) is relatively small (control point 2). (B) Transmembrane water permeability (*Pf*) of the spongy MC can facilitate water export from cells, contributing to transmembrane water flow or moving water toward the cell wall to support apoplastic water flow (control point 3) and transpiration (E, dashed blue line). Note that under optimal conditions, most water flows through the spongy MC, preserving leaf water status (e.g., high Ψ_{leaf} and turgor). (C) Under stressed conditions, high levels of ABA reduce BSC *Pf* (blue dot, control point 1. Shatil-Cohen et al., 2011). In the short term, less water enters the leaf while the amount of water leaving through the stomata remains high, which causes the spongy MC to shrink (Canny et al., 2012) due to their high initial *Pf*, amplifying the stress signal and initiating ABA production (Bacete et al., 2022). Higher ABA then decreases the spongy MC's *Pf* and (D) decreases the transmembrane water flow and apoplast wetting (control points 2 and 3). Diminished flow over the transmembrane and apoplastic water pathways (blue dots and light blue line respectively) keeps water inside the cells, while ABA increases the amount of water transported via the symplastic pathway (red line; control point 2). The effects of all the above combined with the direct effect of ABA on stomata result in reduced K_{leaf} and E (dashed blue line) as leaf water status deteriorates (e.g., reduced Ψ_{leaf} and turgor).

Ache P, Bauer H, Kollist H, Al-Rasheid K a S, Lautner S, Hartung W, Hedrich R (2010) Stomatal action directly feeds back on leaf turgor: new insights into the regulation of the plant water status from non-invasive pressure probe measurements. Plant J **62**: 1072–82

Álvarez-Arenas TEG, Sancho-Knapik D, Peguero-Pina JJ, Gómez-Arroyo A, Gil-Pelegrín E (2018) Non-contact ultrasonic resonant spectroscopy resolves the elastic properties of layered plant tissues. Appl Phys Lett **113**: 1–5

Attia Z, Dalal A, Moshelion M (2019) Vascular bundle sheath and mesophyll cells modulate leaf water balance in response to chitin. Plant J **101:** 1368-1377

Bacete L, Schulz J, Engelsdorf T, Bartosova Z, Vaahtera L, Yan G, Gerhold JM, Ticha T, et al (2022) THESEUS1 modulates cell wall stiffness and abscisic acid production in Arabidopsis thaliana. Proc Natl Acad Sci U S A. **119**: e2119258119

Blackman CJ, Brodribb TJ, Jordan GJ (2010) Leaf hydraulic vulnerability is related to conduit dimensions and drought resistance across a diverse range of woody angiosperms. New Phytol **188**: 1113–1123

Blackman CJ, Brodribb TJ, Jordan GJ (2009) Leaf hydraulics and drought stress: Response, recovery and survivorship in four woody temperate plant species. Plant, Cell Environ **32**: 1584–1595

Blum A (2009) Effective use of water (EUW) and not water-use efficiency (WUE) is the target of crop yield improvement under drought stress. F Crop Res **112**: 119–123

Borsuk AM, Roddy AB, Théroux-Rancourt G, Brodersen CR (2022) Structural organization of the spongy mesophyll. New Phytol **234**: 946–960

Brodribb TJ, Feild TS, Jordan GJ (2007) Leaf Maximum Photosynthetic Rate and Venation Are Linked by Hydraulics. Plant Physiol **144**: 1890–1898

Brodribb TJ, Feild TS, Sack L (2010) Viewing leaf structure and evolution from a hydraulic perspective. Funct Plant Biol **37**: 488–498

Brodribb TJ, Holbrook NM, Zwieniecki MA, Palma B (2005) Leaf hydraulic capacity in ferns, conifers and angiosperms: Impacts on photosynthetic maxima. New Phytol **165**: 839–846

Buckley TN (2015) The contributions of apoplastic, symplastic and gas phase pathways for water transport outside the bundle sheath in leaves. Plant, Cell Environ **38**: 7–22

Buckley TN, John GP, Scoffoni C, Sack L (2015) How does leaf anatomy influence water transport outside the xylem? Plant Physiol **168**: 1616–1635

Canny M (2012) Water loss from leaf mesophyll stripped of the epidermis. Funct Plant Biol

39: 421–434

Canny M, Wong SC, Huang C, Miller C (2012) Differential shrinkage of mesophyll cells in transpiring cotton leaves: Implications for static and dynamic pools of water, and for water transport pathways. Funct Plant Biol **39**: 91–102

Caringella MA, Bongers FJ, Sack L (2015) Leaf hydraulic conductance varies with vein anatomy across Arabidopsis thaliana wild-type and leaf vein mutants. Plant, Cell Environ **38**: 2735-2746.

Christmann A, Hoffmann T, Teplova I, Grill E, Müller A (2005) Generation of active pools of abscisic acid revealed by in vivo imaging of water-stressed arabidopsis. Plant Physiol **137**: 209–219

Clough SJ, Bent AF (1998) Floral dip: A simplified method for Agrobacterium-mediated transformation of Arabidopsis thaliana. Plant J **16**: 735–743

Cochard H, Venisse JS, Barigah TS, Brunel N, Herbette S, Guilliot A, Tyree MT, Sakr S (2007) Putative role of aquaporins in variable hydraulic conductance of leaves in response to light. Plant Physiol **143**: 122–133

Coupel-Ledru A, Tyerman SD, Masclef D, Lebon E, Christophe A, Edwards EJ, Simonneau T (2017) Abscisic acid down-regulates hydraulic conductance of grapevine leaves in isohydric genotypes only. Plant Physiol **175**: 1121–1134

Cui W, Lee JY (2016) Arabidopsis callose synthases *CalS1/8* regulate plasmodesmal permeability during stress. Nat Plants **2**: 1–15

Dalal A, Shenhar I, Bourstein R, Mayo A, Grunwald Y, Averbuch N, Attia Z, Wallach R, Moshelion M (2020) A telemetric, gravimetric platform for real-time physiological phenotyping of plant–environment interactions. J Vis Exp **2020**: 1–28

Erwee MG, Goodwin PB (1984) Characterization of the Egeria densa leaf symplast: Response to plasmolysis, deplasmolysis and to aromatic amino acids. Protoplasma **122**: 162–168

Fischer RA, Rees D, Sayre KD, Lu ZM, Condon AG, Larque Saavedra A (1998) Wheat yield progress associated with higher stomatal conductance and photosynthetic rate, and cooler canopies. Crop Sci **38**: 1467–1475

Galvez-Valdivieso G, Fryer MJ, Lawson T, Slattery K, Truman W, Smirnoff N, Asami T, Davies WJ, Jones AM, Baker NR, et al (2009) The high light response in Arabidopsis involves ABA signaling between vascular and bundle sheath cells. Plant Cell **21**: 2143–62

Griffiths H, Weller G, Toy LFM, Dennis RJ (2013) You’re so vein: Bundle sheath physiology, phylogeny and evolution in C3 and C4 plants. Plant, Cell Environ **36**: 249–261

Grondin A, Rodrigues O, Verdoucq L, Merlot S, Leonhardt N, Maurel C (2015) Aquaporins Contribute to ABA-Triggered Stomatal Closure through OST1-Mediated Phosphorylation. Plant Cell **27**: 1945–1954

Grunwald Y, Wigoda N, Sade N, Yaaran A, Torne T, Gosa SC, Moran N, Moshelion M (2021) Arabidopsis leaf hydraulic conductance is regulated by xylem sap pH, controlled, in turn, by a P-type H^+ -ATPase of vascular bundle sheath cells . Plant J **6**: 301–313

Grunwald Y, Gosa SC, Moran N, Moshelion M (2022) Out of the blue: Phototropins of the leaf vascular bundle sheath mediate the regulation of leaf hydraulic conductance by blue light. Plant Cell **34**: 2328-2342.

Halperin O, Gebremedhin A, Wallach R, Moshelion M (2016) High-throughput physiological phenotyping and screening system for the characterization of plant-environment interactions. Plant J. **89**: 839-850.

Holbrook NM, Shashidhar VR, James R a, Munns R (2002) Stomatal control in tomato with ABA-deficient roots: response of grafted plants to soil drying. J Exp Bot **53**: 1503–14

Iino M, Ogawa T, Zeiger E (1985) Kinetic properties of the blue-light response of stomata. Proc Natl Acad Sci U S A **82**: 8019–8023

Janacek SH, Trenkamp S, Palmer B, Brown NJ, Parsley K, Stanley S, Astley HM, Rolfe SA, Paul Quick W, Fernie AR, et al (2009) Photosynthesis in cells around veins of the C3 plant Arabidopsis thaliana is important for both the shikimate pathway and leaf senescence as well as contributing to plant fitness. Plant J **59**: 329–343

Kelly G, Sade N, Doron-Faigenboim A, Lerner S, Shatil-Cohen A, Yeselson Y, Egbaria A, Kottapalli J, Schaffer AA, Moshelion M, et al (2017) Sugar and hexokinase suppress expression of PIP aquaporins and reduce leaf hydraulics that preserves leaf water potential. Plant J **91**: 325–339

Kemanian AR, Stöckle CO, Huggins DR (2005) Transpiration-use efficiency of barley. Agric For Meteorol **130**: 1–11

Kim YX, Steudle E (2009) Gating of aqaporins by light and reactive oxygen species in leaf parenchyma cells of the midrib of Zea mays. J Exp Bot **60**: 547–556

Kim YX, Steudle E (2007) Light and turgor affect the water permeability (aquaporins) of parenchyma cells in the midrib of leaves of Zea mays. J Exp Bot **58**: 4119–4129

Kitagawa M, Tomoi T, Fukushima T, Sakata Y, Sato M, Toyooka K, Fujita T, Sakakibara H (2019) Abscisic Acid acts as a regulator of molecular trafficking through plasmodesmata in the moss Physcomitrella patens. Plant Cell Physiol **60**: 738–751

Koornneef M, Reuling G, Karssen CM (1984) The isolation and characterization of abscisic acid-insensitive mutants of Arabidopsis thaliana. Physiol Plant **61**: 377–383

Kurihara D, Mizuta Y, Sato Y, Higashiyama T (2015) ClearSee: A rapid optical clearing reagent for whole-plant fluorescence imaging. Dev **142**: 4168–4179

Leegood RC (2008) Roles of the bundle sheath cells in leaves of C3 plants. J Exp Bot **59**: 1663–1673

Lloyd JC, Raines CA, John UP, Dyer TAA (1991) The chloroplast FBPase gene of wheat: structure and expression of the promoter in photosynthetic and meristematic cells of transgenic tobacco plants. MGG Mol Gen Genet **225**: 209–216

Martre P, Morillon R, Barrieu F, North GB, Nobel PS, Chrispeels MJ (2002) Plasma membrane aquaporins play a significant role during recovery from water deficit. Plant Physiol **130**: 2101–2110

Maurel C (1997) Aquaporins and water permeability of plant membranes. Annu Rev Plant Biol **48**: 399–429

McAdam SAM, Brodribb TJ (2016) Linking turgor with ABA biosynthesis: Implications for stomatal responses to vapor pressure deficit across land plants. Plant Physiol **171**: 2008–2016

Merilo E, Yarmolinsky D, Jalakas P, Parik H, Tulva I, Rasulov B, Kilk K, Kollist H (2018) Stomatal VPD response: There is more to the story than ABA. Plant Physiol **176**: 851–864

Morillon R, Chrispeels MJ (2001) The role of ABA and the transpiration stream in the regulation of the osmotic water permeability of leaf cells. Proc Natl Acad Sci U S A **98**: 14138–14143

Muries B, Mom R, Benoit P, Brunel-michac N, Cochard H, Drevet P, Petel G, Badel E, Fumanal B, Gousset-dupont A, et al (2019) Aquaporins and water control in drought-stressed poplar leaves: A glimpse into the extraxylem vascular territories. Environ Exp Bot **162**: 25–37

Nardini A, Gortan E, Salleo S (2005a) Hydraulic efficiency of the leaf venation system in sun- and shade-adapted species. Funct Plant Biol **32**: 953–961

Nardini A, Raimondo F, Lo Gullo MA, Salleo S (2010) Leafminers help us understand leaf hydraulic design. Plant, Cell Environ **33**: 1091–1100

Nardini A, Salleo S, Andri S (2005b) Circadian regulation of leaf hydraulic conductance in sunflower (Helianthus annuus L. cv Margot). Plant, Cell Environ **28**: 750–759

Negin B, Moshelion M (2017) The advantages of functional phenotyping in pre-field screening for drought-tolerant crops. Funct Plant Biol **44**: 107–118

Negin B, Yaaran A, Kelly G, Zait Y, Moshelion M (2019) Mesophyll abscisic acid restrains

early growth and flowering but does not directly suppress photosynthesis. Plant Physiol **180**: 910–925

Pantin F, Monnet F, Jannaud D (2013) The dual effect of abscisic acid on stomata. New Phytol **197**: 65–72

Pilot G, Stransky H, Bushey D (2004) Overexpression of GLUTAMINE DUMPER1 leads to hypersecretion of glutamine from hydathodes of Arabidopsis leaves. Plant Cell **16**: 1827–1840

Pou A, Medrano H, Flexas J, Tyerman SD (2013) A putative role for TIP and PIP aquaporins in dynamics of leaf hydraulic and stomatal conductances in grapevine under water stress and re-watering. Plant, Cell Environ **36**: 828–843

Prado K, Boursiac Y, Tournaire-Roux C, Monneuse J-M, Postaire O, Da Ines O, Schäffner AR, Hem S, Santoni V, Maurel C (2013) Regulation of Arabidopsis leaf hydraulics involves light-dependent phosphorylation of aquaporins in veins. Plant Cell **25**: 1029–39

Prado K, Maurel C (2013) Regulation of leaf hydraulics: from molecular to whole plant levels. Front Plant Sci **4**: 255

Procko C, Lee T, Borsuk A, Bargmann BOR, Dabi T, Nery JR, Estelle M, Baird L, O'Connor C, Brodersen C, et al (2022) Leaf cell-specific and single-cell transcriptional profiling reveals a role for the palisade layer in UV light protection. Plant Cell 1–19

Richards R a (2000) Selectable traits to increase crop photosynthesis and yield of grain crops. J Exp Bot **51**: 447–458

Rockwell FE, Holbrook NM (2017) Leaf hydraulic architecture and stomatal conductance: A functional perspective. Plant Physiol **174**: 1996–2007

Rockwell FE, Holbrook NM, Stroock AD (2014) The competition between liquid and vapor transport in transpiring leaves. Plant Physiol **164**: 1741–58

Sack L, Holbrook NM (2006) Leaf hydraulics. Annu Rev Plant Biol **57**: 361–81

Sack L, John GP, Buckley TN (2018) ABA accumulation in dehydrating leaves is associated with decline in cell volume, not turgor pressure. Plant Physiol **176**: 489–493

Sade N, Shatil-Cohen A, Attia Z, Maurel C, Boursiac Y, Kelly G, Granot D, Yaaran A, Lerner S, Moshelion M (2014) The Role of Plasma Membrane Aquaporins in Regulating the Bundle Sheath-Mesophyll Continuum and Leaf Hydraulics. Plant Physiol **166**: 1609-1620

Sadey N, Shatil-Cohen A, Moshelion M (2015) Bundle-sheath aquaporins play a role in controlling Arabidopsis leaf hydraulic conductivity. Plant Signal Behav **10**: 1–4

Schulz A (1995) Plasmodesmal widening accompanies the short-term increase in symplasmic

phloem unloading in pea root tips under osmotic stress. Protoplasma **188**: 22–37

Scoffoni C, Albuquerque C, Brodersen CR, Townes S V., John GP, Bartlett MK, Buckley TN, McElrone AJ, Sack L (2017) Outside-xylem vulnerability, not xylem embolism, controls leaf hydraulic decline during dehydration. Plant Physiol **173**: 1197–1210

Scoffoni C, Rawls M, Mckown A, Cochard H, Sack L (2011) Decline of leaf hydraulic conductance with dehydration: Relationship to leaf size and venation architecture. Plant Physiol **156**: 832–843

Scoffoni C, Sack L (2017) The causes and consequences of leaf hydraulic decline with dehydration. J Exp Bot **68**: 4479–4496

Scoffoni C, Vuong C, Diep S, Cochard H, Sack L (2014) Leaf shrinkage with dehydration: Coordination with hydraulic vulnerability and drought tolerance. Plant Physiol **164**: 1772–1788

Shapira O, Khadka S, Israeli Y, Shani U, Schwartz A (2009) Functional anatomy controls ion distribution in banana leaves: significance of Na^+ seclusion at the leaf margins. Plant Cell Environ **32**: 476–85

Shatil-Cohen A, Attia Z, Moshelion M (2011) Bundle-sheath cell regulation of xylem-mesophyll water transport via aquaporins under drought stress: a target of xylem-borne ABA? Plant J **67**: 72–80

Shatil-cohen A, Moshelion M (2012) The bundle sheath role as xylem-mesophyll barrier. Plant Signal Behav **7**: 1088–1091

Sinclair TR (2018) Effective water use required for improving crop growth rather than transpiration efficiency. Front Plant Sci **9**: 1–8

Sperry JS, Venturas MD, Anderegg WRL, Mencuccini M, Mackay DS, Wang Y, Love DM (2017) Predicting stomatal responses to the environment from the optimization of photosynthetic gain and hydraulic cost. Plant Cell Environ **40**: 816–830

Steudle E, Peterson C a. (1998) How does water get through roots? J Exp Bot **49**: 775–788

Sussmilch FC, Brodribb TJ, McAdam SAM (2017) Up-regulation of NCED3 and ABA biosynthesis occur within minutes of a decrease in leaf turgor but AHK1 is not required. J Exp Bot **68**: 2913–2918

Tholen D, Boom C, Zhu XG (2012) Opinion: Prospects for improving photosynthesis by altering leaf anatomy. Plant Sci **197**: 92–101

Torne T, Grunwald Y, Dalal A, Yaaran A, Moran N (2021) Stress is basic: ABA alkalinizes both the xylem sap and the cytosol by inhibiting their P-type H^+-ATPase and stimulating their V-type H^+-ATPase. bioRxiv 2021.03.24.436813

Tyree MT, Nardini A, Salleo S, Sack L, El Omari B (2005) The dependence of leaf hydraulic conductance on irradiance during HPFM measurements: any role for stomatal response? J Exp Bot **56**: 737–44

Voicu MC, Cooke JEK, Zwiazek JJ (2009) Aquaporin gene expression and apoplastic water flow in bur oak (Quercus macrocarpa) leaves in relation to the light response of leaf hydraulic conductance. J Exp Bot **60**: 4063–4075

De Wit C (1958) Transpiration and crop yields. Versl Landbouwk Onderz **64 6:** 18–20

Wong SC, Canny MJ, Holloway-phillips M, Stuart-williams H, Cernusak LA, Márquez DA, Farquhar GD (2022) Humidity gradients in the air spaces of leaves. Nat Plants **8**:1-8

Wysocka-Diller JW, Helariutta Y, Fukaki H, Malamy JE, Benfey PN (2000) Molecular analysis of SCARECROW function reveals a radial patterning mechanism common to root and shoot. Development **127**: 595–603

Xiong D, Nadal M (2020) Linking water relations and hydraulics with photosynthesis. Plant J **101**: 800–815

Yaaran A, Moshelion M (2016) Role of aquaporins in a composite model of water transport in the leaf. Int J Mol Sci. **17**: 1045

Yaaran A, Negin B, Moshelion M (2019) Role of guard-cell ABA in determining steady-state stomatal aperture and prompt vapor-pressure-deficit response. Plant Sci **281**: 31–40

Yoo CY, Pence HE, Hasegawa PM, Mickelbart M V. (2009) Regulation of transpiration to improve crop water use. CRC Crit Rev Plant Sci **28**: 410–431

Yoshida T, Christmann A, Yamaguchi-Shinozaki K, Grill E, Fernie AR (2019) Revisiting the basal role of ABA – Roles outside of stress. Trends Plant Sci **24**: 625–635

Zait Y, Shapira O, Schwartz A (2017) The effect of blue light on stomatal oscillations and leaf turgor pressure in banana leaves. Plant Cell Environ **40**: 1143–1152

Zavaliev R, Levy A, Gera A, Epel BL (2013) Subcellular Dynamics and role of Arabidopsis β -1 , 3-Glucanases in cell-to-cell movement of Tobamoviruses. **26**: 1016–1030

Zwieniecki MA, Brodribb TJ, Holbrook NM (2007) Hydraulic design of leaves: Insights from rehydration kinetics. Plant, Cell Environ **30**: 910–921